sustainability

MDPI

Article

Vehicle Driving Behavior Analysis and Unified Modeling in Urban Road Scenarios

Li Zhang [1], Dayi Qu [2,*], Xiaojing Zhang [2], Shouchen Dai [2] and Qikun Wang [2]

[1] School of Information and Control Engineering, Qingdao University of Technology, Qingdao 266520, China
[2] School of Mechanical and Automotive Engineering, Qingdao University of Technology, Qingdao 266520, China
* Correspondence: dayiqu@qut.edu.cn

Abstract: To improve the simulation accuracy and efficiency of microscopic urban traffic, a unified modeling method considering the behavioral characteristics of vehicle drivers is proposed by considering the lane-changing vehicles on the inlet lanes of signalized intersections and their approach following vehicles on the target lanes as research objects. Based on the driver's multidirectional, multi-vehicle anticipation ability and introducing lateral vehicle influence coefficients, the full velocity difference car-following model was extended to microscopic traffic models that consider the driver's capacity for multi-directional, multi-vehicle anticipation. The extended model can describe longitudinal movements of lane changing and car followers using lateral vehicle influential parameters. The influences of traffic control signals and the type of lane change on drivers' decisions were integrated into the model by reformulating the optimal velocity function of the basic car following the model. Similar modeling methods and components were applied to formulate four groups of experimental models and one group of test models. Vehicle trajectory data and manual observations were collected on urban arteries to calibrate and evaluate the research models, experimental models, and test models. The results show that the car-following behavior is more sensitive to the variation in the status of the lateral moving vehicle and change of lane-changing type compared to lane-changing behavior during the lane-changing process. In addition, when lane changing gradually encroaches on the target lane, the vehicle observes the driving conditions and adjusts its driving behaviors differently. This research helps to analyze travel characteristics and influence mechanisms of vehicles on urban roads, which is a guide for the future development of sustainable transportation and self-driving vehicles and promoting the efficient operation of urban transportation systems.

Keywords: driving behavior; unified modeling; car-following model; lane-changing model; sustainable transportation system

check for updates

Citation: Zhang, L.; Qu, D.; Zhang, X.; Dai, S.; Wang, Q. Vehicle Driving Behavior Analysis and Unified Modeling in Urban Road Scenarios. *Sustainability* **2024**, *16*, 1956. https://doi.org/10.3390/su16051956

Academic Editor: Socrates Basbas

Received: 23 December 2023
Revised: 7 February 2024
Accepted: 22 February 2024
Published: 27 February 2024

1. Introduction

Vehicle lane-changing behavior is one of the triggers of macro traffic flow phenomena such as traffic oscillation, capacity drop, and traffic breakdown [1]. The degree of the impact of lane-changing vehicles on neighboring vehicles is directly related to the formation, duration, and dissipation speed of traffic bottlenecks [2]. When simulating lane-changing scenarios with high traffic density, many microscopic traffic flow simulation software outputs abnormal vehicle trajectories, which are usually manifested as lane-changing vehicles "jumping" from the original lane to the target lane, resulting in frequent acceleration and deceleration of the vehicles following behind the two lanes, which triggers abnormal fluctuations in lane traffic flow [3]. This type of problem leads to a decrease in the accuracy of microscopic traffic flow simulation, affecting the reliability of the conclusions of traffic safety evaluation, traffic signal timing, and other aspects of the study based on microscopic traffic flow simulation. The main reason for the above simulation deviation is that the existing microscopic traffic flow model reduces the time continuity of the driving behavior and the driver's ability to respond to changes in the driving environment in a high-density traffic flow environment. From the perspective of model architecture, this defect is mainly manifested with a high degree of separation between the following model and the lane-changing model, as well as insufficient consideration of external factors affecting driver behavior.

Existing studies often decompose continuous vehicle driving actions into two types of sub-behaviors, following and lane changing, and construct relatively independent modeling systems for them [4–11]. The behavioral assumption of this modeling approach is that since the time a driver spends performing a lane change during continuous driving is shorter than the time they spend in a following state, it is assumed that the following behavior is driven by the decision to follow continuously within a certain spatial and temporal range, whereas the lane-changing behavior is derived from the driver's behavioral decision and the time spent on this decision is very short or even negligible. However, in the actual non-free-flow driving scenario, the lane-changing vehicle will continuously adjust its speed and relative position with other vehicles in the pre-lane-changing, mid-lane-changing and post-lane-changing periods to reduce the risk of collision with the neighboring vehicles while creating a suitable space for driving. However, in the actual non-free-flow driving scenario, the lane-changing vehicle will continue to adjust its speed and relative position with other vehicles in the pre-lane-changing, mid-lane-changing and post-lane-changing periods to reduce the risk of collision with the neighboring vehicles while creating a suitable space for driving; in this process, the drivers of the neighboring vehicles who follow the lane-changing vehicle can surmise the other party's intention by observing the movements of the lane-changing vehicle, and continue to adjust the vehicle manipulation behaviors in conjunction with their own driving purpose, so as to weaken the impacts of the changes in the lane-changing vehicle's position on their own. Although only a few studies [12–14] have constructed microscopic traffic flow models to describe the continuous driving actions of lane-changing vehicles, the existing microscopic traffic flow modeling systems of various types do not form a consistent rule on how to switch between the two states of vehicle following and lane changing, which leads to the difficulty of many following models to reflect the continuous impact of lane-changing vehicles on the neighboring and following drivers and the proactive adjustment ability of the following drivers.

In addition, the existing studies have mainly focused on lane-changing behaviors in continuous traffic flow environments, such as urban expressways, and relatively limited research has been conducted on the driving behaviors of individual lane-changing participants in intermittent flow environments, such as urban main roads. Some scholars [1,4] have pointed out that the decision making and behavioral mechanisms of drivers in continuous traffic flow are not fundamentally different from those in intermittent traffic flow, only that the driving environment in the latter is usually more complex, and more factors may affect driver behavior. Therefore, when modeling and analyzing driving behavior in urban road scenarios, it is necessary to choose a basic model that can be considered to be highly scalable for research. Several classical models, such as the optimal velocity (OV) model and the Gipps model, are often extended into microscopic traffic flow models for various driving scenarios [15–19]. Since these models have different assumptions and dynamic characteristics, how to incorporate the influence of external factors on driver behavior into the model by using a reasonable method, in conjunction with the application scenarios, has always been one of the main concerns of micro traffic flow research scholars over the years [20]. Due to the high separation of the existing microscopic traffic flow model system between the following model and the lane-changing model, most models only simulate the behavioral mechanism of a single driver, and the model variables are measured from the driver's perspective, so the calibrated model parameters reflect the behavioral characteristics of a single driver. In addition, the influence of multi-vehicle interaction is more obvious in urban road lane-changing scenarios, and it is necessary to fully understand the influence mechanism of human–vehicle–road multidimensional elements on different drivers and its relationship with macro traffic flow phenomena.

Taking the behaviors of multiple drivers participating in the same lane-changing process on the inlet lane of a signal-controlled intersection of an urban road as the research object, a lane-changing model and a following model with a unified model structure, and without relying on specific following-lane-changing state-switching rules, are established. The effects of intersection signal control as well as lane-changing types are properly incorporated into the model; then, the control and experimental models are constructed in a targeted manner; finally, the various models are calibrated using vehicle trajectory data and manual observations. The effects of intersection signal control as well as lane changing types are appropriately incorporated into the model, the control and experimental models are constructed in a targeted manner, and the vehicle trajectory data and manual observation data are used to calibrate the various types of models. By comparing the performance of various types of models to verify the reasonableness of the basic research models selected in this paper, we understand the influence of external factors on driving behavior during lane changing and their respective driving behavior adjustment methods.

In this study, we improved the accuracy and efficiency of microscopic traffic flow simulations by modeling driving behavior in a unified manner. An in-depth understanding of how following and lane-changing drivers respond to external stimuli and the effects of different research models on model performance was presented. Compared with the existing studies, we investigated the impact of the driving behaviors of different vehicles in the surrounding lanes on the characteristics of drivers in this lane by considering the impact of traffic signal control and the impact of lane changing of vehicles in the adjacent lanes through four sets of experimental models and test models. The results showed that the vehicle-following behavior is significantly affected by lateral vehicles, and this study has positive significance for further parsing vehicle-following behavior in real-world scenarios.

Through the comparative study of drivers' longitudinal and lateral influences, the traffic characteristics of urban traffic flow are explored, and the influence mechanism is provided to help improve the operational efficiency of urban traffic flow, which in turn contributes to the realization of green urban transportation and sustainable development. This study on drivers' influencing factors is an effective way to reveal the operating characteristics of urban traffic flow and is also a basic method for the rational construction of urban traffic models.

2. Driver Behavior Analysis

2.1. Driving Scene Interaction Relationships

Figure 1 shows the relationship between space positions and distances during vehicle driving and lane changing, in which the interactions among the lane-changing vehicle (LCV), the potential following vehicle (PFV) in the target lane, and the potential leading vehicle (PLV) are more significant. Therefore, the three driver behaviors are selected as the object of study. Since the LCV and PFV are always traveling behind the PLV, it is assumed that the PLV driver is not affected by both, but the actions of the PLV will affect the LCV and PFV driver's decisions. As the lane-changing initiator, the LCV driver needs to decide the position and timing of lateral insertion based on the traveling conditions of the PLV and PFV. The adjustment maneuver of the PFV driver in response to the LCV insertion directly affects the motion state of the following vehicle, and the magnitude of its adjustment determines the degree of disturbance to the traffic flow in the target lane by the lane-changing vehicle. Similar to the PFV driver, the LCV driver during the lane changing is affected by the changes in the traveling states of the remaining two vehicles that are parallel and perpendicular to the lane direction. Microscopic traffic flow modeling in various driving scenarios is usually carried out based on the classical following model. Since the basic model already can simulate the longitudinal driving characteristics of vehicles, one of the main concerns of this study is how to introduce the effects of sideways-moving vehicles on drivers into the model.

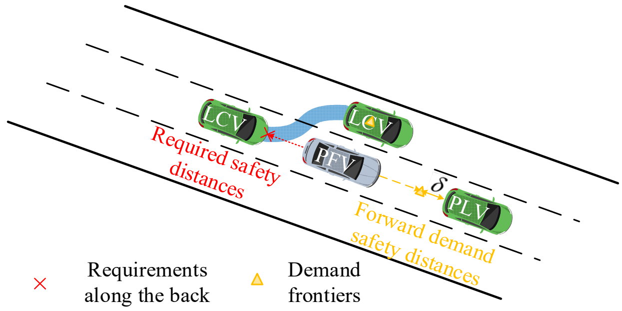

Figure 1. Interaction relationship of vehicle-vehicle.

2.2. The Effect of Sideways-Moving Vehicles on Driving Behavior

2.2.1. Following Model Considering the Effect of Sideways Vehicles

It has been found that roadway geometric factors, such as insufficient lane lateral clearance or excessive lane width, affect the longitudinal driving stability of following vehicles [21]. In recent years, some scholars have begun to model and analyze the behaviors of following drivers in response to the cross-traffic vehicles in front of them. Gunay [22] simulated the following driver by modifying the Gipps model to avoid the deceleration of the vehicle in front by using the gap in this lane or using adjacent lanes to bypass the front vehicle's avoidance-driving behavior and analyzed the effects of lane width on following speed and the degree of offset between the two vehicles on following distance. Jin et al. [23,24] incorporated the effect of lateral spacing between the front and rear vehicles into the expanded healing model by refining the GM and OV models. He et al. [25] investigated the following behavior under the combined effect of vehicle lateral spacing and driver-overtaking intention. In contrast, Li et al. [26] considered the effect of bilateral spacing between the front and rear vehicles on the following driver. The above studies mainly incorporate the lateral angle between the front and rear vehicles as a variable in the following model to simulate the influence of sideways moving vehicles, then use numerical simulation to analyze the influence of the change of angle on the stability of the follower model and the macroscopic traffic flow, and fewer studies carried out empirical analyses based on actual data.

2.2.2. Lane-Changing Model Considering the Effect of Sideways Vehicles

Most of the lane-changing models contain variables reflecting changes in the state of vehicles traveling laterally in the target lane; however, existing studies mainly focus on the lane-changing decision mechanisms of LCV drivers in the target lane under the influence of PFV and PLV as well as their lane-changing preparatory actions in the original lane. Only a few studies have constructed microscopic traffic flow models that can completely depict lane-changing preparation and insert the target lane until the completion of the lane changing and other sequential actions. As early representatives of research in this direction, Moridpour et al. [12] simulated the longitudinal acceleration and deceleration behaviors of a lane-changing vehicle during the whole process of traveling from the original lane to the target lane by extending the GM model:

$$\begin{cases} c_i(t+\tau_i) = \mu_0 v_i(t+\tau_i)^{\mu_1} \frac{[v_{i+1}(t)-v_i(t)]^{\mu_2}}{[x_{i-1}(t)-x_i(t)]^{\mu_3}} \\ d_i(t+\tau_i) = \mu_0 v_i(t+\tau_i)^{\mu_1} \frac{[v_{i+2}(t)-v_i(t)]^{\mu_2}}{[x_{i-1}(t)-x_i(t)]^{\mu_3}} \end{cases} \tag{1}$$

where $v_i(t)$, $v_{i+2}(t)$, $v_{i-1}(t)$, and $v_{i-1}(t)$ are the vehicle speeds of vehicle i, $i+1$, $i+2$, and $i-1$ in Figure 1 at the time t, respectively; $x_{i-1}(t)$ and $x_i(t)$ are the positions of the vehicle $i-1$ and i at the time t, respectively; $c_i(t+\tau_i)$ and $d_i(t+\tau_i)$ are the longitudinal acceleration and deceleration of the lane-changing vehicle i at the time $t+\tau_i$, respectively; τ_i is the reaction time of the driver of the vehicle i; and μ_0, μ_1, μ_2, and μ_3 are the coefficients to be calibrated. However, this model still has some defects, for example, the change of vehicle spacing when the speed difference is zero does not affect $c_i(t+\tau_i)$ and $d_i(t+\tau_i)$, and the effect of the vehicle $i-1$ on the driver of the vehicle i is not considered. Based on the longitudinal speed and steering angle of the lane-changing vehicle i, its lateral speed is determined. The time-varying lateral influence coefficients are introduced to simulate the effects of the vehicle $i+2$ and $i-2$ on the longitudinal acceleration of the vehicle i, using the OV model as a basis:

$$v_i(t+\tau_i) = \theta_i(t)v_{i-1}(t+\tau_i) + [1-\theta_i(t)]v_{i-2}(t+\tau_i) \quad (2)$$

where $v_{i-1}(t+\tau_i)$ and $v_{i-2}(t+\tau_i)$ are the speed adjustment values calculated by the lane-changing driver at moment $t+\tau_i$ using the OV model based on the movements of vehicles $i-1$ and $i-2$ at moment t, respectively; $\theta_i(t)$ is used to characterize the influence weights of vehicles $i-1$ and $i-2$ on the lane-changing driver. The lane-changing scenarios are categorized into cooperative lane changing and forced lane changing. In the collaborative lane-changing scenario, the model structure of Equation (2) is followed to modify the Gipps model to describe the longitudinal driving action of lane-changing vehicles i. The forced lane changing scenario further extends Equation (2) as:

$$v_i(t+\tau_i) = \theta_i(t)v_{i-1}(t+\tau_i) + [1-\theta_i(t)]\{\varphi_i(t)v_{i-2}(t+\tau_i) + [1-\varphi_i(t)]v_{i+2}(t+\tau_i)\} \quad (3)$$

where: $v_{i+2}(t+\tau_i)$ is the adjusted speed of the lane-changing driver at the moment $t+\tau_i$ according to the action of the vehicle t. The lateral influence coefficient characterizes the influence weights of the vehicle $i-2$ and the lane-changing driver.

Changes in inter-vehicle angle and the degree of lateral vehicle intrusion were used to simulate the impact of lateral vehicle driving state changes on driver behavior, respectively. It is more difficult for drivers to accurately measure angle changes than distance changes under real driving conditions.

2.3. Driver Multidirectional Multi-Vehicle Anticipation Capability

2.3.1. Characterization

Existing lane-changing models all take into account the effect of the multi-vehicle travel states in the original and target lanes on lane-changing drivers. Empirical studies have found that following drivers have the “multi-vehicle anticipation ability” to predict the future driving conditions of the vehicle in front of them in their lane [15]. Still, recent studies have shown that this ability is not limited to the single-lane category [27]. This driving skill, which is possessed by both the following driver and the lane-changing driver, can be referred to as “multidirectional multi-vehicle anticipation capability”. Specifically, in the vehicle–vehicle interaction scenario shown in Figure 1, this ability is characterized by the following features in PFV drivers and LCV drivers:

1. Frequency

In collaborative lane-changing scenarios, PFV will actively decelerate before the LCV enters the target lane to create a larger insertion gap for the LCV [3]. However active slowing is not the only way for PFV drivers to deal with the effects of LCV, and driving behavior can be influenced by the traffic environment in which they operate. For example, when PFV and LCV are in stop-and-go startup traffic, both drivers expect that neighboring vehicles will need to accelerate away from the intersection in the short term, in which case the PFV driver observes a lower probability of active deceleration when the LCV moves sideways and is more likely to maintain a uniform or even accelerated speed. Therefore, it is reasonable to assume that the multidirectional multi-vehicle anticipation capability of PFV drivers comes into play in all lane-changing scenarios.

2. Gradual and Shared

PFV drivers need to observe PLV and LCV continuously for a while before they can judge their driving intentions and gradually form stable expectations about their future driving conditions. In addition, since the risk of collision between the LCV or

PFV and neighboring vehicles exists simultaneously, drivers of both vehicles need to continuously observe the driving conditions of other vehicles and adjust their driving behavior accordingly. Therefore, it is reasonable to assume that the multidirectional multi-vehicle anticipatory capabilities of the drivers of both vehicles develop gradually and function simultaneously during the lane-changing process.

2.3.2. Interactive Relationship

The traveling relationship among PLV, LCV, and PFV in Figure 1 is summarized in Figure 2: PFV and LCV form a pair of lane-changing groups, PFV and PLV constitute a couple of longitudinal following groups, as well as LCV and PLV as a pair of lateral following groups. The influence of neighboring vehicles on a PFV or LCV driver can be decomposed into two directions, perpendicular and parallel to the lane. Since LCV can complete lane changing by crossing only one lane, it is assumed that LCV drivers have better control over the degree of vehicle lateral drift, and that PFV drivers can accurately observe the degree of LCV lateral drift. Lane-changing scenarios can be subdivided into three categories: overrunning lane changing, yielding lane changing, and general lane changing, as shown in Figure 3a–c. To ensure that the multidirectional multi-vehicle anticipation abilities of LCV and PFV drivers functioned simultaneously during the study period, the starting and ending moments of the lane-changing process in the three types of scenarios ($t = 1$) were defined as the moments when the front bumpers of the PFV and LCV were flush, the rear bumpers of the PLV and LCV were flush, and the LCV turn signals turned on or the front end started to shift sideways, respectively. The end moment of lane changing ($t = n$) is uniformly defined as the moment when the body of the LCV returns to the parallel state with the lane divider after entering the target lane. The above definition will be used to process the vehicle trajectory data extracted from urban road traffic flow videos.

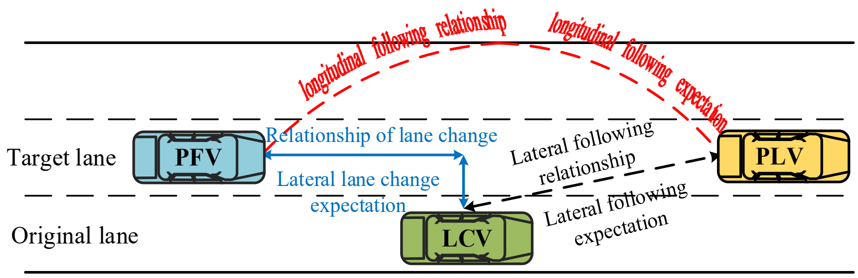

Figure 2. Interactions relationships of three main participants during the lane-changing process.

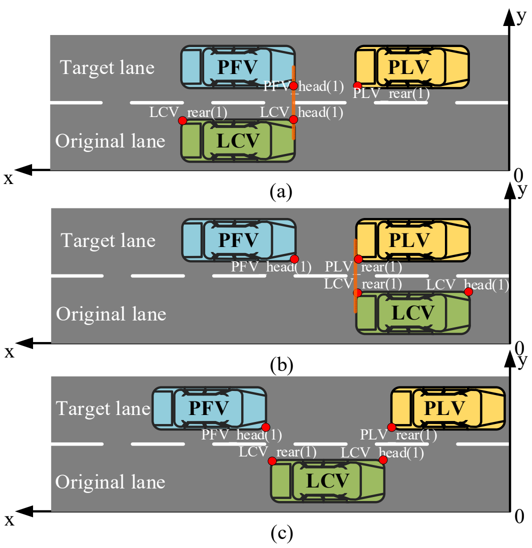

Figure 3. Start of lane changing (t = 1) at the scenario of overtaking (**a**), overtaken (**b**), or normal (**c**) lane changing.

3. Experimental Program and Data Collection

A section of the Haier expressway in Qingdao City, with a length of about 220 m, a speed limit of 60 km/h, and signalized intersections upstream and downstream, was selected as the study site. It is assumed that the drivers on the roadway can observe the downstream intersection signals. Traffic flow videos of the study roadway are collected on roadside high-rise buildings and vehicle trajectories are extracted. A total of 250 sets of vehicle trajectory data are collected, and the collection points of each set of data include the front corner points of PFV, the rear corner points of PLV, and the front and rear corner points of LCV shown in Figure 3, with a sampling frequency of 10 Hz. At the same time, the intersection signal color and the lane-changing type of the target vehicle were manually observed on the roadside. The trajectory data were calibrated using an algorithm suitable for urban road environments [28], and the speed values extracted from the data were compared with those obtained from the radar speedometer to verify the accuracy of the trajectory data extraction. Figure 4 shows the study section and the control points used for calibration of the trajectory data. Figure 5 shows the trajectories of LCV moving vertically in the direction of the lanes in Vehicle Group 126 (left graph) and Vehicle Group 134 (right graph), that is, the correspondence between the vertical coordinate y and time in Figure 3. The former stayed in the original lane for a longer period and made repeated trials as well as positional adjustments (before 4 s) before moving smoothly into the target lane, a process that lasted about 7 s. The latter changed from the right to the left lane, a process that lasted about 5 s. The lateral movement was relatively smooth, and finding or creating an insertable gap did not take a long time. Variables extracted from vehicle trajectories in both horizontal and vertical directions as well as from manual observations will be used in microscopic traffic flow modeling.

Figure 4. Data acquisition of the vehicle and trajectory.

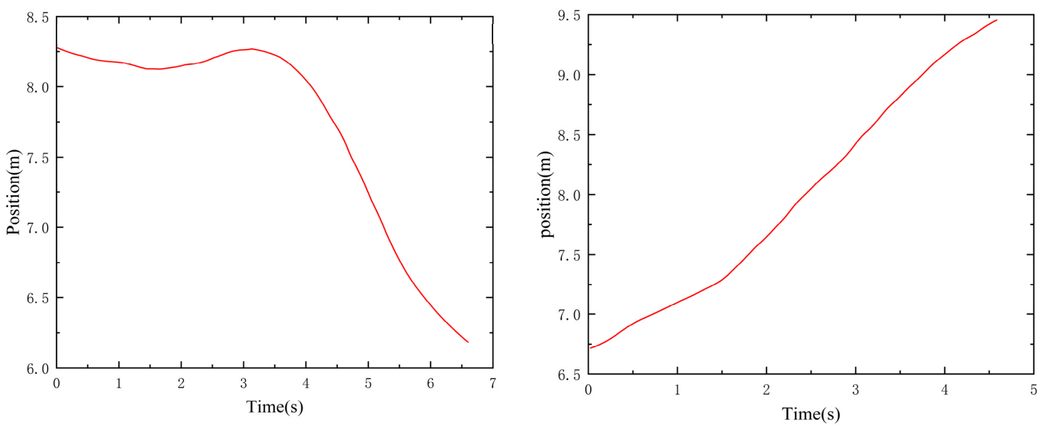

(**a**) The position of vehicle group 126. (**b**) The position of vehicle group 134.

Figure 5. The lateral moving trajectory of the vehicle.

4. Unified Modeling of Driving Behavior

4.1. Driving Behavior Model

Vehicles traveling on the inlet road of urban road intersections have the characteristics of low average speed and frequent acceleration or deceleration. It is found that the full velocity difference (FVD) model can better simulate the nonlinear acceleration or deceleration actions of vehicles than the Gipps model and the OV model [29], so this model is chosen as the basis for modeling the longitudinal driving actions of LCV and PFV uniformly in the process of changing lanes. The structure of the FVD model is as follows:

$$a_i(t) = \beta_i\{V_i[\Delta x_i(t)] - v_i(t)\} + \lambda_i \Delta v_i(t) \tag{4}$$

where $a_i(t)$ is the acceleration of the vehicle i at time t; $\Delta x_i(t)$ is the headway between the vehicle i and the vehicle in front of it at the time t; $v_i(t)$ is the speed of the vehicle i at time t; $V_i(.)$ is the optimized speed function identified by the driver of the vehicle i; β_i is the sensitivity coefficient of the driver of the vehicle i to the difference between $V_i(.)$ and $v_i(t)$; $\Delta v_i(t)$ is the speed difference between vehicle i and the vehicle in front of it; λ_i is the sensitivity of the driver of the vehicle i to $\Delta v_i(t)$. The FVD model can be extended to a longitudinal multi-vehicle following a model that takes into account the reaction time of the driver and the influence of the multi-vehicle ahead:

$$a_i(t+\tau_i) = \beta_i\left\{V_i\left[\sum_{j=1}^{J} \delta_j \Delta x_{ij}(t)\right] - v_i(t)\right\} + \sum_{j=1}^{J} \lambda_j \Delta v_{ij}(t) \tag{5}$$

where J is the number of vehicles ahead affecting vehicle i; $\Delta x_{ij}(t)$ is the spacing between vehicle i and vehicle j at the time t; δ_j is the coefficient of influence of $\Delta x_{ij}(t)$ on the driver of the vehicle i, and the sum of all δ_j is 1; $\Delta v_{ij}(t)$ is the speed difference between vehicle i and vehicle j at the time t; λ_j is the coefficient of influence of $\Delta v_{ij}(t)$ on the driver of the vehicle i, and the sum of all λ_j is 1; $V_i(.)$ is defined as [17]:

$$V_i[\Delta x_i(t)] = V_{i1} + V_{i2}\tanh[C_{i1}\Delta x_i(t) - C_{i2}] \tag{6}$$

where V_{i1}, V_{i2}, C_{i1}, and C_{i2} are the parameters to be calibrated.

4.2. Following Model

The longitudinal multi-vehicle following model is transformed into a following model that takes into account the combined effects of driver multidirectional multi-vehicle expectancy capacity, traffic signals, and lane-changing type:

$$a_{\mathrm{PFV}}(t+\tau_{\mathrm{PFV}}) = \beta_{\mathrm{PFV}}\{V_{\mathrm{PFV}}[F_{\mathrm{PFV}\Delta x}(.)] - v_{\mathrm{PFV}}(t)\} + F_{\mathrm{PFV}\Delta v}(.) \tag{7}$$

where τ_{PFV} is the reaction time of the PFV driver; $a_{\mathrm{PFV}}(t+\tau_{\mathrm{PFV}})$ is the longitudinal acceleration of the PFV at the moment $t+\tau_{\mathrm{PFV}}$; $\Delta vLCV$ and $\Delta vPLV$ are the velocity differences between the PFV and the LCV or PLV, respectively; $V_{\mathrm{PFV}}(.)$ is the optimized speed function of the following driver; β_{PFV} is the sensitivity coefficient of the following driver to the difference between the speed $v_{\mathrm{PFV}}(t)$ and the optimized speed $v_{\mathrm{PFV}}(.)$ at the moment t. The vehicle spacing variable function $F_{\mathrm{PFV}\Delta x}(.)$ and the velocity difference variable function $F_{\mathrm{PFV}\Delta v}(.)$ of the green light phase period following model are defined as:

$$\begin{cases} F_{\mathrm{PFV}\Delta x}(.) = \xi_{\Delta x\mathrm{LCV}}\theta_{\mathrm{PFV}}(t)\Delta x_{\mathrm{LCV}}(t) + \xi_{\Delta x\mathrm{PLV}^*}[1-\theta_{\mathrm{PFV}}(t)]\Delta x_{\mathrm{PLV}^*}(t) \\ F_{\mathrm{PFV}\Delta v}(.) = \xi_{\Delta v\mathrm{LCV}}\theta_{\mathrm{PFV}}(t)\Delta v_{\mathrm{LCV}}(t) + \xi_{\Delta v\mathrm{PLV}^*}[1-\theta_{\mathrm{PFV}}(t)]\Delta v_{\mathrm{PLV}^*}(t) \end{cases} \tag{8}$$

where $\theta_{\mathrm{PFV}}(t)$ is the lateral influence coefficient of the following model; $\Delta x_{\mathrm{LCV}}(t)$ and $\Delta x_{\mathrm{PLV}^*}(t)$ are the distance between the PFV and the LCV or PLV at time t, respectively; $\Delta v_{\mathrm{LCV}}(t)$ and $\Delta v_{\mathrm{PLV}^*}(t)$ are the speed difference between the PFV and the LCV or PLV at time t, respectively. From the definition of A, it can be seen that when the LCV enters the target lane, its effect on the PFV driver gradually increases, while the effect of the PLV on the PFV driver gradually decreases. The exact form of b will depend on the model calibration results:

$$\begin{cases} \theta_{\mathrm{PFV1}}(t) = k_{\mathrm{PFV}} \cdot P_{\mathrm{LCV}}(t) \\ \theta_{\mathrm{PFV2}}(t) = \tan[P_{\mathrm{LCV}}(t)]/k_{\mathrm{PFV}} \\ \theta_{\mathrm{PFV3}}(t) = \tanh[P_{\mathrm{LCV}}(t)]/k_{\mathrm{PFV}} \end{cases} \tag{9}$$

where k_{PFV} is the parameter to be calibrated; the lateral deviation $P_{\mathrm{LCV}}(t)$ is defined in Equation (10). The definition of the red-light phase period is as follows:

$$F_{\mathrm{PFV}\Delta x}(.) = \xi_{\Delta x\mathrm{LCV}}\theta_{\mathrm{PFV}}(t)\Delta x_{\mathrm{LCVs}}(t) + \xi_{\Delta x\mathrm{PLV}^*}[1-\theta_{\mathrm{PFV}}(t)]\Delta x_{\mathrm{PLVs}}(t) \tag{10}$$

where $\Delta x_{\mathrm{LCVs}}(t)$ is the distance between the LCV and the parking line at the moment t. Similarly, using the forced lane-changing scenario as a baseline, the sensitivity coefficients ($\xi_{\Delta x\mathrm{LCV}}$ and $\xi_{\Delta x\mathrm{PLV}^*}$) of PFV drivers to their spacing with the LCV or PLV as well as the sensitivity coefficients ($\xi_{\Delta v\mathrm{LCV}}$ and $\xi_{\Delta v\mathrm{PLV}^*}$) of the speed difference in the active lane-changing scenario satisfy the following constraints:

$$\begin{cases} \xi_{\Delta x\mathrm{LCV}} + \xi_{\Delta x\mathrm{PLV}^*} = 1 \\ \xi_{\Delta v\mathrm{LCV}} + \xi_{\Delta v\mathrm{PLV}^*} = 1 \end{cases} \tag{11}$$

4.3. Lane-Changing Model

Drawing on the modeling approaches of Wang et al. [13] and Yang et al. [14], the longitudinal multi-vehicle following model shown in Equation (5) is transformed into a lane-changing model that takes into account the multidirectional multi-vehicle anticipation capability of LCV drivers while influencing factors such as traffic control signals and lane-changing types are introduced into the model:

$$a_{\mathrm{LCV}}(t+\tau_{\mathrm{LCV}}) = \beta_{\mathrm{LCV}}\{V_{\mathrm{LCV}}[F_{\mathrm{LCV}\Delta x}(.)] - v_{\mathrm{LCV}}(t)\} + F_{\mathrm{LCV}\Delta v}(.) \tag{12}$$

where $a_{\mathrm{LCV}}(t+\tau_{\mathrm{LCV}})$ is the longitudinal acceleration of the LCV driver at the moment $t+\tau_{\mathrm{LCV}}$; τ_{LCV} is the reaction time of the LCV driver; β_{LCV} is the sensitivity coefficient of the LCV driver to the difference between the vehicle speed $v_{\mathrm{LCV}}(t)$ and the optimized speed $V_{\mathrm{LCV}}(.)$ at the moment t; the vehicle spacing variable function $F_{\mathrm{LCV}\Delta x}(.)$ and the vehicle speed difference variable function $F_{\mathrm{LCV}\Delta v}(.)$ are defined as follows:

$$\begin{cases} F_{\mathrm{LCV}\Delta x}(.) = \xi_{\Delta x\mathrm{PFV}}\theta_{\mathrm{LCV}}(t)\Delta x_{\mathrm{PFV}}(t) + \xi_{\Delta x\mathrm{PLV}}[1-\theta_{\mathrm{LCV}}(t)]\Delta x_{\mathrm{PLV}}(t) \\ F_{\mathrm{LCV}\Delta v}(.) = \xi_{\Delta v\mathrm{PFV}}\theta_{\mathrm{LCV}}(t)\Delta v_{\mathrm{PFV}}(t) + \xi_{\Delta v\mathrm{PLV}}[1-\theta_{\mathrm{LCV}}(t)]\Delta v_{\mathrm{PLV}}(t) \end{cases} \tag{13}$$

where $\theta_{\mathrm{LCV}}(t)$ is the lateral influence coefficient in the lane-changing model; $\Delta x_{\mathrm{PFV}}(t)$ and $\Delta x_{\mathrm{PLV}}(t)$ are the distance between LCV and PFV or PLV at moment t, respectively; $\Delta v_{\mathrm{PFV}}(t)$ and $\Delta v_{\mathrm{PLV}}(t)$ are the velocity differences between LCV and PFV or PLV at moment t, respectively. Equation (8) describes the following driving scenario: as the LCV moves progressively into the target lane, the LCV driver is progressively less influenced by the PFV and gradually more influenced by the PLV. The specific form of A will be selected from Equation (9) based on the lane-changing model calibration results:

$$\begin{cases} \theta_{\mathrm{LCV1}}(t) = k_{\mathrm{LCV}} \cdot P_{\mathrm{LCV}}(t) \\ \theta_{\mathrm{LCV2}}(t) = \tan[P_{\mathrm{LCV}}(t)]/k_{\mathrm{LCV}} \\ \theta_{\mathrm{LCV3}}(t) = \tanh[P_{\mathrm{LCV}}(t)]/k_{\mathrm{LCV}} \end{cases} \tag{14}$$

where $\tan(.)$ and $\tanh(.)$ are the tangent and hyperbolic tangent functions, respectively; k_{LCV} is the parameter to be calibrated; $P_{\mathrm{LCV}}(t)$ is the lateral offset of the LCV at the time t:

$$P_{\mathrm{LCV}}(t) = \left| \frac{y_{\mathrm{LCV\_h}}(t) - y_{\mathrm{LCV\_h}}(n)}{\max[y_{\mathrm{LCV\_h}}(t)] - \min[y_{\mathrm{LCV\_h}}(t)]} \right| \tag{15}$$

where $y_{\mathrm{LCV\_h}}(t)$ is the longitudinal coordinate of the LCV head angle point (point *LCV_head* in Figure 3) at time t; n is the end of lane change; $\max[y_{\mathrm{LCV\_h}}(t)]$ and $\min[y_{\mathrm{LCV\_h}}(t)]$ are the maximum and minimum values of $y_{\mathrm{LCV\_h}}(t)$, respectively. The definition of the denominator of Equation (10) ensures that $P_{\mathrm{LCV}}(t)$ still reflects the degree of lateral excursion of the LCV when the lateral movement distance of the LCV is greater or less than the lane width.

The influence of traffic control signals on LCV drivers is mainly reflected in their judgment of the future driving trends of neighboring vehicles. PFV, LCV, and PLV all pass through the intersection as quickly as possible during the green light phase, while they all need to slow down and stop during the red-light phase. LCV drivers adjust their expectation of vehicle speed according to this trend, and this behavioral mechanism can be described by adjusting the optimized speed function $V_{LCV}(.)$ in the vehicle spacing variable combination function $F_{\mathrm{LCV}\Delta x}(.)$ to describe it. $F_{\mathrm{LCV}\Delta x}(.)$, defined by Equation (8), is still followed in the green phase period, i.e., it is assumed that the optimized speed of the LCV depends on its spacing from the PFV and PLV. Assume that the desired speed of the LCV in the red-light phase period depends on the distances of the PFV and PLV from the stop line at the moment t. The definitions of both are shown in Figure 6. x_{safe} is the safe distance between the two vehicles at a complete stop, and L is the length of the vehicle body, at which time the definition is modified to:

$$F_{\mathrm{LCV}\Delta x}(.) = \xi_{\Delta x\mathrm{PFV}}\theta_{\mathrm{LCV}}(t)\Delta x_{\mathrm{PFVs}}(t) + \xi_{\Delta x\mathrm{PLV}}[1-\theta_{\mathrm{LCV}}(t)]\Delta x_{\mathrm{PLVs}}(t) \tag{16}$$

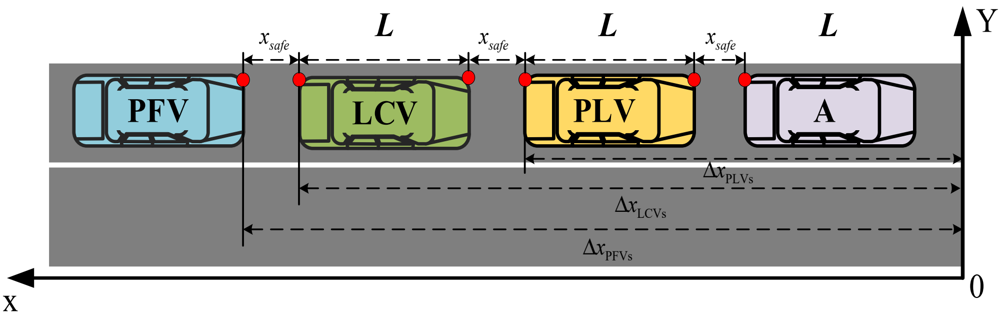

Figure 6. Vehicle queuing status at signalized intersection.

The effects of different types of lane changing on drivers' behavior are mainly reflected in the intensity of their vehicle maneuvers. According to the classification of drivers' lane-changing objectives, they can be categorized into discretionary lane changing to obtain a higher speed or a shorter queue, and mandatory lane changing to drive to the destination. As the initiator of the lane change, the LCV driver knows the purpose of their lane change, and the PFV driver can obtain this information by comparing the LCV's original lane with the target lane flow. The willingness of mandatory lane-changing drivers is usually stronger than that of discretionary lane-changing drivers. Using the mandatory lane-changing scenario as a baseline, the sensitivity coefficients ($\xi_{\Delta x\mathrm{PFV}}$ and $\xi_{\Delta x\mathrm{PLV}}$) of discretionary lane-changing drivers to their spacing from the PFV and PLV and the sensitivity coefficients ($\xi_{\Delta v\mathrm{PFV}}$ and $\xi_{\Delta v\mathrm{PLV}}$) of the speed difference satisfy the following constraints, respectively:

$$\begin{cases} \xi_{\Delta x\mathrm{PFV}} + \xi_{\Delta x\mathrm{PLV}} = 1 \\ \xi_{\Delta v\mathrm{PFV}} + \xi_{\Delta v\mathrm{PLV}} = 1 \end{cases} \tag{17}$$

5. Model Calibration and Evaluation

5.1. Model Calibration

The model calibration is divided into three main steps:

1. Selecting the driver reaction times A and B in the lane changing and following model;
2. Selecting the calculation methods for the lateral influence coefficients C and D;
3. Calibrating the remaining parameters in the model. In the first two steps, all of the study data were used for parameter calibration. In the third step, 200 sets of data were

randomly selected for model calibration and another 50 sets of data were used for model performance testing.

The parameter calibration work for the lane changing and following models can be abstracted as solving a nonlinear optimization problem, where constraints can be set according to the physical range of values of each parameter. Then, the gap between the actual vehicle position, velocity, or acceleration and the model predictions is minimized. The Theil function is chosen as the optimization objective function, and the applicability of this function in the calibration of microscopic traffic flow models has been verified by previous studies [19,29]:

$$U = \frac{\sqrt{\sum_{m=1}^{M}(a_{\text{real\_}m} - a_{\text{sim\_}m})^2}}{\sqrt{\sum_{m=1}^{M}(a_{\text{real\_}m})^2} + \sqrt{\sum_{m=1}^{M}(a_{\text{sim\_}m})^2}} \tag{18}$$

where $a_{\text{real\_}m}$ and $a_{\text{sim\_}m}$ are the longitudinal acceleration of the vehicle calculated using the original data and the simulation model, respectively; m is the sample number of the data, and M is the total number of samples; U is the inequality coefficient of the Theil function, and the closer U is to zero the better the model fits the real data. The ranges of the values of the parameters to be calibrated in the lane-changing model and the following model are listed in Table 1. The genetic algorithm toolbox of MATLAB is used to solve this optimization problem, and the algorithm parameters are set in reference [30]: population size 50; maximum number of iterations 300; crossover probability 0.8; migration interval 20; migration probability 0.2; initial penalty factor 10; minimum error 10^{-6}.

Table 1. Value range of model parameters.

The Following Model				
Parameter name	β_{PFV}	k_{PFV}	$\xi_{\Delta xLCV}$	$\xi_{\Delta xPLV^*}$
Range of values	(0,1)	(0,10)	(0,1)	(0,1)
Parameter name	$\xi_{\Delta vLCV}$	$\xi_{\Delta vPLV^*}$	V_{PFV1}	V_{PFV2}
Range of values	(0,1)	(0,1)	(−30,30)	(−40,40)
Parameter name	C_{PFV1}	C_{PFV2}		
Range of values	(−10,10)	(−10,10)		
Lane-Changing Model				
Parameter name	β_{LCV}	k_{LCV}	$\xi_{\Delta x\text{PFV}}$	$\xi_{\Delta x\text{PLV}}$
Range of values	(0,1)	(0,10)	(0,1)	(0,1)
Parameter name	$\xi_{\Delta v\text{PFV}}$	$\xi_{\Delta v\text{PLV}}$	V_{LCV1}	V_{LCV2}
Range of values	(0,1)	(0,1)	(−30,30)	(−40,40)
Parameter name	C_{LCV1}	C_{LCV2}		
Range of values	(−10,10)	(−10,10)		

5.2. Model Evaluation

5.2.1. Evaluation Indicator

The performance of the calibrated model was evaluated using the metrics of Mean Error (ME), Mean Absolute Error (MAE), and Root Mean Square Error (RMSE), which were calculated for each metric:

$$\begin{cases} ME = \frac{1}{M}\sum_{m=1}^{M}(a_{\text{real\_}m} - a_{\text{sim\_}m}) \\ MAE = \frac{1}{M}\sum_{m=1}^{M}|a_{\text{real\_}m} - a_{\text{sim\_}m}| \\ RMSE = \sqrt{\frac{1}{M}\sum_{m=1}^{M}(a_{\text{real\_}m} - a_{\text{sim\_}m})^2} \end{cases} \tag{19}$$

5.2.2. Experimental Model

First, four sets of test models are constructed. Then, by comparing the evaluation results of the research model and the experimental model, we can understand the way lane-changing drivers and following drivers cope with the influence of external factors.

Experimental lane-changing model 1 and experimental following model 1: Assuming that LCV drivers and PFV drivers only consider each other's longitudinal traveling state, while not taking into account the effects of the degree of lateral offset, PLV traveling state, and changes in the type of lane changing, Equations (8) and (14) become:

$$\begin{cases} F_{\text{LCV}\Delta x}(.) = \Delta x_{\text{PFV}}(t),\ F_{\text{LCV}\Delta v}(.) = \Delta v_{\text{PFV}}(t) \\ F_{\text{PFV}\Delta x}(.) = \Delta x_{\text{LCV}}(t), F_{\text{PFV}\Delta v}(.) = \Delta v_{\text{LCV}}(t) \end{cases} \tag{20}$$

Experimental lane-changing model 2 and experimental following model 2: it is assumed that LCV drivers and PFV drivers are affected by the side traveling vehicles and the change of lane-change type, but the effect of PLV motion state is not considered, Equations (8) and (14) become:

$$\begin{cases} F_{\text{LCV}\Delta x}(.) = \xi_{\Delta x\text{PFV}}\theta_{\text{LCV}}(t)\Delta x_{\text{PFV}}(t) \\ F_{\text{LCV}\Delta v}(.) = \xi_{\Delta v\text{PFV}}\theta_{\text{LCV}}(t)\Delta v_{\text{PFV}}(t) \\ F_{\text{PFV}\Delta x}(.) = \xi_{\Delta x\text{LCV}}\theta_{\text{PFV}}(t)\Delta x_{\text{LCV}}(t) \\ F_{\text{PFV}\Delta v}(.) = \xi_{\Delta v\text{LCV}}\theta_{\text{PFV}}(t)\Delta v_{\text{LCV}}(t) \end{cases} \tag{21}$$

Experimental lane-changing model 3 and experimental following model 3: assuming that both LCV drivers and PFV drivers are only concerned with the PLV traveling state in the target lane, Equations (8) and (14) become:

$$\begin{cases} F_{\text{LCV}\Delta x}(.) = \xi_{\Delta x\text{PLV}}[1-\theta_{\text{LCV}}(t)]\Delta x_{\text{PLV}}(t) \\ F_{\text{LCV}\Delta v}(.) = \xi_{\Delta v\text{PLV}}[1-\theta_{\text{LCV}}(t)]\Delta v_{\text{PLV}}(t) \\ F_{\text{PFV}\Delta x}(.) = \Delta x_{\text{PLV}}(t) \\ F_{\text{PFV}\Delta v}(.) = \Delta v_{\text{PLV}^*}(t) \end{cases} \tag{22}$$

Experimental lane-changing model 4 and experimental following mode 4: assuming that LCV drivers and PFV drivers are not affected by the change in lane-change type, Equations (8) and (14) becomes:

$$\begin{cases} F_{\text{LCV}\Delta x}(.) = \theta_{\text{LCV}}(t)\Delta x_{\text{PFV}}(t) + [1-\theta_{\text{LCV}}(t)]\Delta x_{\text{PLV}}(t) \\ F_{\text{LCV}\Delta v}(.) = \theta_{\text{LCV}}(t)\Delta v_{\text{PFV}}(t) + [1-\theta_{\text{LCV}}(t)]\Delta v_{\text{PLV}}(t) \\ F_{\text{PFV}\Delta x}(.) = \theta_{\text{PFV}}(t)\Delta x_{\text{LCV}}(t) + [1-\theta_{\text{PFV}}(t)]\Delta x_{\text{PLV}^*}(t) \\ F_{\text{PFV}\Delta v}(.) = \theta_{\text{PFV}}(t)\Delta v_{\text{LCV}}(t) + [1-\theta_{\text{PFV}}(t)]\Delta v_{\text{PLV}^*}(t) \end{cases} \tag{23}$$

5.2.3. Comparison Model

The modeling method from Yang et al. [14] was used to construct the comparison lane-changing model and the comparison following model, then by comparing the evaluation results of the experimental model 4 and the comparison model, the effect of the difference in the performance of the base model on the research results can be obtained. The comparison lane-changing model is:

$$v_{\text{LCV}}(t+\tau_{\text{LCV}}) = \theta_{\text{LCV}}v_{\text{PFV}}(t+\tau_{\text{LCV}}) + (1-\theta_{\text{LCV}})v_{\text{PLV}}(t+\tau_{\text{LCV}}) \tag{24}$$

where: $v_{\text{PLV}}(t+\tau_{\text{LCV}})$ and $v_{\text{PFV}}(t+\tau_{\text{LCV}})$ are defined as:

$$v_{\text{PLV}}(t+\tau_{\text{LCV}}) = d_{\text{LCV}}\tau_{\text{LCV}} + \sqrt{(d_{\text{LCV}}\tau_{\text{LCV}})^2 - d_{\text{LCV}}\begin{bmatrix} 2\Delta x_{\text{LCV/PLV}}(t) - v_{\text{LCV}}(t)\tau_{\text{LCV}} \\ -v_{\text{PLV}}^2(t)/d_{\text{PLV}} \end{bmatrix}} \tag{25}$$

$$v_{\text{PFV}}(t+\tau_{\text{LCV}}) = 0.5d_{\text{LCV}}\tau_{\text{LCV}} + \sqrt{(0.5d_{\text{LCV}}\tau_{\text{LCV}})^2 + d_{\text{LCV}}\begin{bmatrix} 2\Delta x_{\text{LCV/PFV}}(t) + v_{\text{LCV}}(t)\tau_{\text{LCV}} \\ -2v_{\text{PFV}}(t)\tau_{\text{LCV}} + v_{\text{PFV}}^2(t)/d_{\text{PFV}} \end{bmatrix}} \tag{26}$$

where d_{LCV}, d_{PLV}, and d_{PFV} are the maximum deceleration of LCV, PLV, and PFV, respectively, the range of values of d_{LCV} is set to (−11.2, −3), the range of values of d_{PLV} and

d_{PFV} is set to (−13, −3), and all units are $\text{m} \cdot \text{s}^2$. Although Yang et al. [14] did not state the modeling method for PFV driver behavior in their study, it is still possible to draw on their methodology to construct a comparison of the following model:

$$v_{\text{PFV}}(t+\tau_{\text{PFV}}) = \theta_{\text{PFV}} v_{\text{LCV}}(t+\tau_{\text{PFV}}) + (1-\theta_{\text{PLV}}) v_{\text{PLV}}(t+\tau_{\text{PFV}}) \tag{27}$$

where $v_{\text{LCV}}(t+\tau_{\text{PFV}})$ and $v_{\text{PLV}}(t+\tau_{\text{PFV}})$ are defined as:

$$v_{\text{LCV}}(t+\tau_{\text{PFV}}) = d_{\text{PFV}}\tau_{\text{PFV}} + \sqrt{(d_{\text{PFV}}\tau_{\text{PFV}})^2 - d_{\text{PFV}}\begin{bmatrix} 2\Delta x_{\text{PFV/LCV}}(t) - v_{\text{PFV}}(t)\tau_{\text{PFV}} \\ -v_{\text{LCV}}^2(t)/d_{\text{LCV}} \end{bmatrix}} \tag{28}$$

$$v_{\text{PLV}}(t+\tau_{\text{PFV}}) = d_{\text{PFV}}\tau_{\text{PFV}} + \sqrt{(d_{\text{PFV}}\tau_{\text{PFV}})^2 - d_{\text{LCV}}\begin{bmatrix} 2\Delta x_{\text{PFV/PLV}}(t) - v_{\text{PFV}}(t)\tau_{\text{PFV}} \\ -v_{\text{PLV}}^2(t)/d_{\text{PLV}} \end{bmatrix}} \tag{29}$$

5.3. Model Evaluation

5.3.1. Evaluation Indicator

Since the trajectory data are collected at a frequency of 10 Hz and the driver's minimum reaction time is usually not shorter than 0.2 s, the candidate values of τ_{LCV} and τ_{PFV} are substituted into the lane-changing model and the follow-along model one by one in intervals between 0.2 s and 1 s and at intervals of 0.1 s. By comparing the values of the Theil function U computed by the model calibration, the values of τ_{LCV} and τ_{PFV} with the highest fit to the original data are searched for. The results in Table 2 show that when $\tau_{LCV} = 1$ s and $\tau_{PFV} = 0.7$ s, the lane-changing model and the following model have the highest fit. Since τ_{PFV} is smaller than τ_{LCV}, it can be seen that the sensitivity of PFV drivers to external stimuli during lane changing is higher than that of LCV drivers.

Table 2. Driver's reaction time.

Driver Reaction Time (s)	$U(\tau_{LCV}(t))$	$U(\tau_{PFV}(t))$
0.2	0.6022	0.6389
0.3	0.5994	0.6392
0.4	0.5964	0.6422
0.5	0.6017	0.6380
0.6	0.5964	0.6369
0.7	0.6031	0.6301
0.8	0.6003	0.6313
0.9	0.5987	0.6341
1.0	0.5886	0.6326

5.3.2. Lateral Influence Coefficient

Based on τ_{LCV} and τ_{PFV}, the calculations of the lateral influence coefficients $\theta_{\text{LCV}}(t)$ and $\theta_{\text{PFV}}(t)$ are selected from Equations (9) and (15), then introduced into the lane-changing and following models. The specific forms of $\theta_{\text{LCV}}(t)$ and $\theta_{\text{PFV}}(t)$ are determined by comparing the U values calculated using the different forms. The calculations in Table 3 show that $\theta_{\text{LCV3}}(t)$ and $\theta_{\text{PFV1}}(t)$ have the best fit. Therefore, they will be used subsequently to calibrate the remaining parameters:

$$\begin{cases} \theta_{\text{LCV}}(t) = \tanh[P_{\text{LCV}}(t)]/k_{\text{LCV}} \\ \theta_{\text{PFV}}(t) = k_{\text{PFV}} \cdot P_{\text{LCV}}(t) \end{cases} \tag{30}$$

Table 3. Lateral influencing parameter.

$\boldsymbol{\theta}_{\mathbf{LCV}}(\boldsymbol{t})$	$\boldsymbol{U}(\boldsymbol{\theta}_{\mathbf{LCV}}(\boldsymbol{t}))$	$\boldsymbol{\theta}_{\mathbf{PFV}}(\boldsymbol{t})$	$\boldsymbol{U}(\boldsymbol{\theta}_{\mathbf{PFV}}(\boldsymbol{t}))$
entry 1	0.5900	$\theta_{\mathrm{PFV1}}(t)$	0.6360
$\theta_{\mathrm{LCV2}}(t)$	0.5923	$\theta_{\mathrm{PFV2}}(t)$	0.6384
$\theta_{\mathrm{LCV3}}(t)$	0.5834	$\theta_{\mathrm{PFV3}}(t)$	0.6419

Figure 7 shows the lateral offset $P_{\mathrm{LCV}}(t)$, relative to $\theta_{\mathrm{LCV}}(t)/\theta_{\mathrm{PFV}}(t)$. Combining the definitions of the two, shows that the closer the LCV is to the end position of the changeover, the smaller $P_{\mathrm{LCV}}(t)$ becomes, which causes the values of $\theta_{\mathrm{LCV}}(t)$ and $\theta_{\mathrm{PFV}}(t)$ to gradually decrease and approach each other. From the definitions of the lane-changing model in Equation (7) and the following model in Equation (13), it can be seen that a decrease implies that the LCV driver is progressively less affected by the PFV and progressively more affected by the PLV; decreasing $\theta_{\mathrm{PFV}}(t)$ means that the PFV driver is progressively less affected by the PLV and progressively more affected by the LCV. Combining Figure 7 and the definitions of the two models shows that the effect of the LCV on the PFV driver increases linearly as the LCV gradually enters the target lane. In addition, the influence of PFV on the LCV driver decreases slowly ("LCV" curve slope is small) at the beginning of the lane changing (larger interval of $P_{\mathrm{LCV}}(t)$ value in Figure 7), indicating that the LCV driver is still continuously concerned about the movement state of PFV at this stage; when the LCV is near the terminal point of the lane changing (smaller interval of $P_{\mathrm{LCV}}(t)$ value in Figure 7), the influence of PFV on the LCV driver decreases rapidly ("LCV" curve slope increases in Figure 7), and near the finish of the lane changing, the LCV driver is affected only by the PLV. This result indicates that LCV drivers mainly focus on the state of the PFV before entering the target lane and turn to pay more attention to the state of the PLV after entering the target lane.

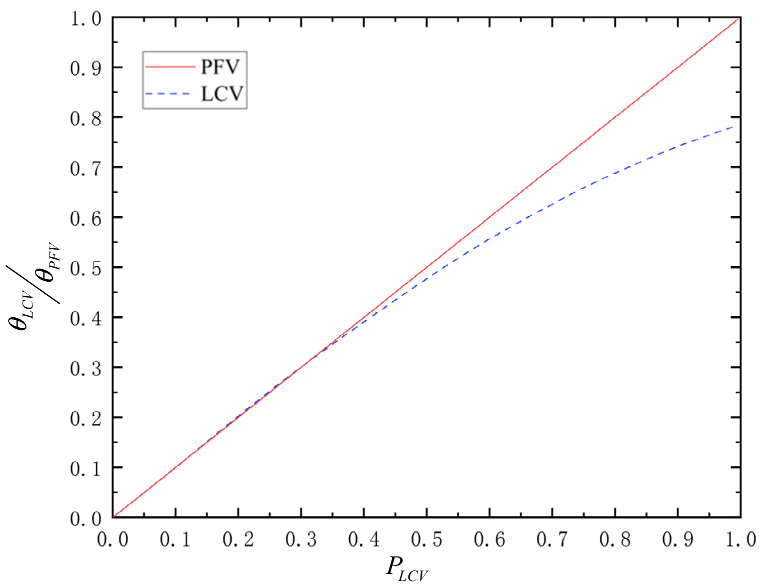

Figure 7. Relationships between $P_{LCV}(t)$ and $\theta_{LCV}(t)/\theta_{PFV}(t)$.

5.3.3. Other Parameters

The selected driver reaction time and lateral influence coefficients are substituted into the lane-changing model and the following model to calibrate the other parameters in the model, and the results are shown in Table 4. Comparing the values of β_{PFV} and β_{LCV}, it can be seen that the PFV driver is more sensitive to the difference between the optimal speed and the current speed ($\beta_{PFV} = 0.114 > \beta_{LCV} = 0.086$). Since this coefficient is equal to the reciprocal of the driver reaction time [16], this result indirectly verifies the reasonableness of the driver's reaction time setting in Section 5.3.1. In addition, lane-changing scenarios change the attention of both drivers to external stimuli. Compared to the mandatory lane-changing scenario, LCV drivers in the discretionary lane-changing scenario paid more attention to their spacing from the PLV than to their spacing from the PFV ($\xi_{\Delta xPFV} = 0.241 < \xi_{\Delta xPLV} = 0.759$), and LCV drivers in this scenario are more affected by their speed difference with the PFV than by their speed difference with the PLV ($\xi_{\Delta vPFV} = 0.601 > \xi_{\Delta vPLV} = 0.398$). This means that the LCV driver in the discretionary lane-changing scenario mainly ensures safe driving by regulating the spacing with the PLV or the speed difference with the PFV. Similarly, it can be seen that the PFV driver in the discretionary lane-changing scenario mainly avoids the traveling risk by adjusting its spacing and speed difference with the PLV ($\xi_{\Delta xLCV} = 0.344 < \xi_{\Delta xPLV^*} = 0.656$; $\xi_{\Delta vLCV} = 0.129 < \xi_{\Delta vPLV^*} = 0.869$).

Table 4. Results of model calibration.

The Following Model				
Parameter name	β_{PFV}	k_{PFV}	$\xi_{\Delta xLCV}$	$\xi_{\Delta xPLV^*}$
Calibration result	0.114	0.218	0.344	0.656
Parameter name	$\xi_{\Delta vLCV}$	$\xi_{\Delta vPLV^*}$	V_{PFV1}	V_{PFV2}
Calibration result	0.129	0.869	−20.245	25.840
Parameter name	C_{PFV1}	C_{PFV2}		
Calibration result	1.055	5.249		
Lane-Changing Model				
Parameter name	β_{LCV}	k_{LCV}	$\xi_{\Delta x\mathrm{PFV}}$	$\xi_{\Delta x\mathrm{PLV}}$
Calibration result	0.086	0.942	0.241	0.759
Parameter name	$\xi_{\Delta v\mathrm{PFV}}$	$\xi_{\Delta v\mathrm{PLV}}$	V_{LCV1}	V_{LCV2}
Calibration result	0.601	0.398	7.637	36.938
Parameter name	C_{LCV1}	C_{LCV2}		
Calibration result	0.285	0.543		

5.4. Results of Model Evaluation

The models in Equations (7) and (13) are referred to as the study lane-changing model and the study healing model, respectively, and the results of the evaluation of each model are shown in Table 4, which show that the fit and accuracy of each model perform well. In the study of the lane-changing model, the research lane-changing model has the lowest average error, which indicates that the model considering the combined effects of driver's multidirectional multi-vehicle anticipation ability, traffic signals, and lane-changing types is more consistent with the real data, and the extended full-speed-difference model can better simulate the vehicle operation status on urban roads than the Gipps lane-changing model. In the lane-changing model study, the average error of the experimental following model 2 is significantly smaller than that of the other models, indicating that drivers are significantly affected by the changes in side-traveling vehicles and lane-changing types, and are more in line with the real-world scenarios.

Experimental model 1 assumes that LCV drivers and PFV drivers adjust their driving behaviors based on each other's longitudinal travel status only, while experimental model 2 considers the effects of the other's lateral motion status and lane-changing type changes on drivers. It is worth noting that when the above two factors are considered in the model, the improvement effect of the experimental following model is more obvious than that of the experimental lane-changing model (ME, lane-changing model: $|1.185–1.024| <$ following mode $|1.200–1.082|$; MAE, lane-changing model: $|2.987–2.585| <$ following mode: $|3.366–2.677|$; RMSE, lane-changing model: $|3.732–3.249| <$ following mode: $|4.157–3.333|$). The model evaluation results in Table 5 show that the experimental lane-changing model 2 outperforms the experimental lane-changing model 1 (lane-changing model 1: $|-1.185|/2.987/3.723 >$ lane-changing model 2: $|-1.024|/2.585/3.249$). This result suggests that the effects of lateral moving vehicles and changes in lane-changing type are more significant for PFV drivers than for LCV drivers, and also sides with the finding that PFV drivers are more sensitive to external disturbances than LCV drivers during lane-changing as described in Section 5.3.1.

Table 5. Results of model evaluation.

The Following Model			
Evaluation of indicators	ME	MAE	RMSE
Research following model	0.404	3.279	4.142
Experimental following model 1	1.200	3.366	4.187
Experimental following model 2	1.082	2.677	3.333
Experimental following model 3	2.095	3.659	4.367
Experimental following model 4	0.856	3.296	4.223
Comparison with the following model	1.476	3.643	4.357
Lane-Changing Model			
Evaluation of indicators	ME	MAE	RMSE
Research lane-changing model	−1.10	2.572	3.290
Experimental lane-changing model 1	−1.185	2.987	3.723
Experimental lane-changing model 2	−1.024	2.585	3.249
Experimental lane-changing model 3	−2.667	3.689	4.569
Experimental lane-changing model 4	−1.143	2.580	3.437
Comparison with the lane-changing model	−1.768	2.589	4.432

Experimental model 3 assumes that LCV drivers and PFV drivers will only be affected by PLV and will not pay attention to each other's driving status, whereas the situation described in the experimental following model 3 is a common setup in existing micro traffic flow simulation software [3]. The results show that the performance of experimental model 3 is worse than that of experimental model 1 and 2 (lane-changing model, ME: $|-2.667| > |-1.185| > |-1.024|$, MAE: 3.689 > 2.987 > 2.585, RMSE: 4.569 > 3.723 > 3.249; following mode, ME: 2.095 > 1.200 > 1.082, MAE: 3.659 > 3.366 > 2.677, RMSE: 4.367 > 4.187 > 3.333). Neglecting the lateral vehicle moving state has a more significant effect on the performance of the lane-changing model than the following model.

The above results indicate that LCV drivers and PFV drivers do adjust their driving behaviors according to each other's driving conditions, and if the microscopic traffic flow simulation software ignores this behavioral feature, the phenomenon of frequent emergency braking output from the simulation model may occur, which affects the reliability of the simulation results. The experimental model 4 and the comparison model have the same model structure, with the difference is that they are extended from the FVD model and the Gipps model, respectively. The results of the model evaluation show that the comparison model fits the actual data less well than the experimental model 4 (lane-changing model, ME: $|-1.768| > |-1.143|$, MAE: 2.589 > 2.580, RMSE: 4.432 > 3.437; following mode, ME: 1.467 > 0.856, MAE: 3.643 > 3.296, RMSE: 4.357 > 4.223). This result suggests that the FVD model can better describe the microscopic driving behavior in urban road traffic flow compared to the Gipps model. Since the proposed model mainly takes into account the influence of driving behavior of adjacent lanes on driver characteristics, and the urban road traffic environment is complex and variable, the effects of traffic congestion and road urbanization need to be fully considered in subsequent research sinks to improve the applicability of the model.

6. Conclusions

Vehicle following and lane-changing behaviors can each anticipate multidirectional multi-vehicle driving conditions, and driving behaviors are modeled uniformly to improve the accuracy and efficiency of microscopic traffic flow simulation. Based on the full speed difference following model, it is expanded into a lane changing model and a following model that considers the driver's ability to anticipate multi-directional multi-vehicle conditions, and factors such as traffic control signals and lane-changing types are incorporated into the model. Overall, four sets of experimental models and one set of comparison models were constructed using a similar approach. Since the models are structurally uniform, comparing the parameters of the different models provides insights into how following and lane-changing drivers respond to external stimuli and the effects of the different underlying research models on model performance.

Compared with lane-changing behavior, the following behavior is more sensitive to external stimuli. As the lane-changing vehicle gradually enters the target lane, its effect on the following driver increases linearly, while the effect of the following vehicle on the lane-changing driver lasts longer. Driving behavior's focus on external stimuli changes with lane-changing scenarios.

Considering the effect of sideways moving vehicles in the lane-changing model and the following model significantly improves the model performance. The effects of changes in the lateral vehicle motion and lane change type were stronger for the following driver than for the LCV driver. The extended full-speed difference model simulates vehicle driving conditions on urban roads better than the Gipps following model.

The follow-up study will adopt a unified driving behavior modeling approach to adapt the classical car-following models, such as the GM model and the IDM model, to better understand the applicability of different base models in multidimensional traffic scenarios by comparing the model performances. Since vehicle type and size are important factors affecting drivers' driving, as well as factors such as different road conditions and intersections also affecting drivers' operating behavior, we will fully consider the impact of vehicle type on the optimization of the model in this study, as well as the impact of urban traffic organization on driver characteristics in the follow-up study to further improve the applicability of the model.

Author Contributions: Conceptualization, L.Z. and D.Q.; methodology, L.Z.; software, X.Z. and S.D.; validation, D.Q., X.Z. and Q.W.; investigation, S.D. and Q.W.; writing—original draft preparation, L.Z.; writing—review and editing, D.Q. All authors have read and agreed to the published version of the manuscript.

Funding: This research was funded by the National Natural Science Foundation of China: 52272311.

Institutional Review Board Statement: This study did not require ethical approval.

Informed Consent Statement: Written informed consent has been obtained from the patient(s) to publish this paper.

Data Availability Statement: We have no right to disclose the data used in this study.

Conflicts of Interest: The authors declare no conflicts of interest.

References

1. Zhou, M.F.; Yu, Y.; Qu, X.B. Development of an efficient driving strategy for connected and automated vehicles at signalized intersections: A reinforcement learning approach. *IEEE Trans. Intell. Transp. Syst.* **2020**, *21*, 433–443. [CrossRef]
2. Zhang, R.X.; Masoud, S.; Masoud, N. Impact of Autonomous Vehicles on the Car-Following Behavior of Human Drivers. *J. Transp. Eng. Part A Syst.* **2022**, *149*, 1–25. [CrossRef]
3. Chen, Q.; Zhou, Y.; Ahn, S.; Xia, J.; Li, S.; Li, S. Robustly string stable longitudinal control for vehicle platoons under communication failures: A generalized extended state observer-based control approach. *IEEE Trans. Intell. Veh.* **2022**, *8*, 159–171. [CrossRef]
4. Guo, H.B.; Qu, D.Y.; Hong, J.L.; Zhao, Z.X.; Hei, K.X. Vehicle lane changing interaction behavior and decision model based on utility theory. *Sci. Technol. Eng.* **2020**, *20*, 12185–12190.
5. Sharma, A.; Zheng, Z.; Kim, J.; Bhaskar, A.; Haque, M.M. Assessing traffic disturbance, efficiency, and safety of the mixed traffic flow of connected vehicles and traditional vehicles by considering human factors. *Transp. Res. Part C Emerg. Technol.* **2021**, *124*, 102934. [CrossRef]
6. Gong, B.; Wang, F.; Lin, C.; Wu, D. Modeling HDV and CAV Mixed Traffic Flow on a Foggy Two-Lane Highway with Cellular Automata and Game Theory Model. *Sustainability* **2022**, *14*, 5899. [CrossRef]
7. Kesting, A.; Treiber, M.; Helbing, D. General lane changing model MOBIL for car following models. *Transp. Res. Rec. J. Transp. Res. Board* **2007**, *1999*, 86–94. [CrossRef]
8. Negash, N.M.; Yang, J. Driver behavior modeling towards autonomous vehicles: Comprehensive review. *IEEE Access* **2023**, *11*, 22788–22821. [CrossRef]

9. Li, L.; Zhang, D.; Xu, Z.G.; Wang, P.; Wang, G.P. The roles of car following and lane changing drivers' anticipations during vehicle inserting process: A structural equation model approach. *J. Adv. Transp.* **2018**, *2018*, 1–19. [CrossRef]
10. Gao, Y.; Levinson, D. Lane changing and congestion are mutually reinforcing. *Commun. Transp. Res.* **2023**, *3*, 100101. [CrossRef]
11. Chen, K.; Knoop, V.L.; Liu, P.; Li, Z.; Wang, Y. Modeling the impact of lane-changing's anticipation on car-following behavior. *Transp. Res. Part C Emerg. Technol.* **2023**, *150*, 104110. [CrossRef]
12. Moridpour, S.; Sarvi, M.; Rose, G. Modeling the lane changing execution of multiclass vehicles under heavy traffic conditions. *Transp. Res. Rec. J. Transp. Res. Board* **2010**, *46*, 11–19. [CrossRef]
13. Wang, H.; Li, Y.; Wang, W. Modeling lane changing execution on the basis of car following theory. In Proceedings of the Transportation Research Board, Transportation Research Board 94th Annual Meeting, Washington, DC, USA, 11–15 January 2015.
14. Yang, D.; Zhu, L.L.; Ran, B.; Pu, Y.; Hui, P. Modeling and analysis of the lane changing execution in longitudinal direction. *IEEE Trans. Intell. Transp. Syst.* **2016**, *17*, 1–9. [CrossRef]
15. Nirmale, S.K.; Pinjari, A.R.; Sharma, A. A discrete-continuous multi-vehicle anticipation model of driving behaviour in heterogeneous disordered traffic conditions. *Transp. Res. Part C Emerg. Technol.* **2021**, *128*, 103144. [CrossRef]
16. Montanino, M.; Punzo, V. On string stability of a mixed and heterogeneous traffic flow: A unifying modelling framework. *Transp. Res. Part B Methodol.* **2021**, *144*, 133–154. [CrossRef]
17. Wang, Z.; Huang, H.; Tang, J.; Meng, X.; Hu, L. Velocity control in car-following behavior with autonomous vehicles using reinforcement learning. *Accid. Anal. Prev.* **2022**, *174*, 106729. [CrossRef] [PubMed]
18. Zhao, J.; Knoop, V.L.; Wang, M. Microscopic traffic modeling inside intersections: Interactions between drivers. *Transp. Sci.* **2023**, *57*, 135–155. [CrossRef]
19. Li, M.; Fan, J.; Lee, J. Modeling Car-Following Behavior with Different Acceptable Safety Levels. *Sustainability* **2023**, *15*, 6282. [CrossRef]
20. Han, J.; Wang, X.; Wang, G. Modeling the Car-Following Behavior with Consideration of Driver, Vehicle, and Environment Factors: A Historical Review. *Sustainability* **2022**, *14*, 8179. [CrossRef]
21. Gunay, B. Methods to quantify the discipline of lane-based driving. *Traffic Eng. Control* **2003**, *44*, 22–27.
22. Gunay, B. Car following theory with lateral discomfort. *Transp. Res. Part B Methodol.* **2007**, *41*, 722–735. [CrossRef]
23. Jin, S.; Wang, D.H.; Yang, X.R. Non-lane-based car following model using visual angle information. *Transp. Res. Rec. J. Transp. Res. Board* **2011**, *2249*, 7–14. [CrossRef]
24. Jin, S.; Wang, D.H.; Xu, C.; Huang, Z.Y. Staggered car following induced by lateral separation effects in traffic flow. *Phys. A Stat. Mech. Its Appl.* **2012**, *376*, 153–157. [CrossRef]
25. He, Z.C.; Wang, Y.M.; Sun, W.B.; Huang, P.Y.; Zhang, L.C.; Zhong, R.X. Modelling car following behavior with lateral separation and overtaking expectation. *Transp. B Transp. Dyn.* **2016**, *4*, 223–239.1.
26. Li, Y.F.; Zhang, L.; Peeta, S.; Pan, H.G.; Zheng, T.X.; Li, Y.G.; He, X.Z. Non-lane-discipline-based car following model considering the effects of two-sided lateral gaps. *Nonlinear Dyn.* **2015**, *80*, 227–238. [CrossRef]
27. Choudhury, C.F.; Islam, M.M. Modelling acceleration decisions in traffic streams with weak lane discipline: A latent leader approach. *Transp. Res. Part C* **2016**, *67*, 214–226. [CrossRef]
28. Arun, A.; Haque, M.M.; Washington, S.; Mannering, F. A physics-informed road user safety field theory for traffic safety assessments applying artificial intelligence-based video analytics. *Anal. Methods Accid. Res.* **2023**, *37*, 100252. [CrossRef]
29. Punzo, V.; Simonelli, F. Analysis and comparison of microscopic traffic flow models with real traffic microscopic data. *Transp. Res. Rec. J. Transp. Res. Board* **2005**, *1934*, 53–63. [CrossRef]
30. Li, L.; Chen, X.Q.; Zhang, L. A Global Optimization algorithm for trajectory data based car following model calibration. *Transp. Res. Part C* **2016**, *68*, 311–332. [CrossRef]